# Analysis of tunable diode laser spectra of the $\nu_4$ band of $^{12}C_3{}^{16}O_2$

W. H. Weber and P. D. Maker

*Physics Department, Engineering and Research Staff, Ford Motor Company, Dearborn, Michigan 48121*

C. W. Peters

*Physics Department, University of Michigan, Ann Arbor, Michigan 48104*
(Received 25 September 1975)

Current-tunable thin-film PbTe diode lasers have been used to obtain Doppler-limited resolution of the $\nu_4$ asymmetric stretch band of $C_3O_2$ in the region 1565–1600 $cm^{-1}$. Roughly 70% of the interval was covered using different modes of three lasers, each mode giving a tuning range of 1–3 $cm^{-1}$. Absolute spectral calibration was obtained from $NH_3$ and $H_2O$, together with the channel spectrum of a 4-cm Ge etalon recorded simultaneously using a double beam technique. Rotational constants were determined for the $\nu_4$ fundamental band and five different hot bands associated with the thermally excited low frequency bending mode $\nu_7$. The band origin for the ground state transition is 1587.390±0.002 $cm^{-1}$ and the $\nu_7$ hot bands are shifted progressively to lower frequency. The systematic shift of the hot bands was verified independently with temperature difference spectra from a Fourier transform spectrometer.

## I. INTRODUCTION

We describe in this paper the use of tunable, thin-film, PbTe diode lasers in a study of the $\nu_4$ fundamental band of $C_3O_2$ in the region 1565–1610 $cm^{-1}$. Diode lasers made from Pb–salt semiconductors have been used previously in several spectroscopic studies exploiting their high spectral impurity.[1] Some examples are studies of Λ-type doubling,[2,3] pressure broadening,[4,5] Zeeman splittings,[2] Stark splittings,[6] and nuclear hyperfine splittings.[7] In each of these experiments the spectra obtained covered a range of at most only a few $cm^{-1}$. The work reported here is on the use of such lasers in the analysis of vibration–rotation bands in an extended spectral region of roughly 35 $cm^{-1}$. From spectra recorded with Doppler-limited resolution, the fundamental and five different hot bands of $\nu_4$ of $C_3O_2$ have been identified, rotational constants for all of these bands have been determined, and over 300 lines have been assigned.

The fundamental vibrational frequencies of $C_3O_2$ are known fairly well from extensive Raman and infrared studies.[8–14] The last fundamental to be observed directly was the lowest frequency bending vibration $\nu_7$ reported by Carriera *et al.*[15] to be at 22 $cm^{-1}$. The present of this low frequency mode leads to a large number of hot bands associated with transitions whose lower states have one or more quanta of $\nu_7$ thermally excited. Except in some of the combination bands in the near infrared, these hot bands tend to completely overlap one another, greatly complicating any attempts at rotational analyses. There has, in fact, been no previous analysis of rotational structure in any of the fundamentals of this molecule.

The first infrared study of $C_3O_2$ resolving the rotational structure was made on an unidentified combination band near 3200 $cm^{-1}$ by Lafferty, Maki, and Plyler.[16] They provided convincing evidence that the molecule's structure is linear with $D_{\infty h}$ symmetry and obtained molecular constants from analyses of a $\Sigma-\Sigma$ and a $\Pi-\Pi$ series. Recently, Mantz *et al.*[17] have re-examined the near infrared spectrum using a Fourier transform spectrometer with much higher resolution. They analyzed rotational structure in seven different $\Sigma-\Sigma$ bands and confirmed the assignment by Lafferty *et al.* of the 3169 $cm^{-1}$ band as orginating in the ground vibrational state. Different values for the ground state molecular constants were obtained by Mantz *et al.*,[17] however, which they attributed to a misassignment of the $J$ values in the earlier work.

We present results of analyses of the vibration–rotation spectrum of the $\nu_4$ fundamental (species $\sigma_u$), which is the asymmetric C=C=C stretching mode. All of the observed transitions are of the type $\nu_4$ 1 ← 0 with a lower level having 0, 1, or 2 quanta of $\nu_7$ (species $\pi_u$) thermally excited. Thus the bands will be of the type $\Sigma_u-\Sigma_g$, $\Pi_g-\Pi_u$, or $\Delta_u-\Delta_g$. Because of spin statistics, the $\Sigma-\Sigma$ bands will contain only even $J$'s, while the remaining bands will have both even and odd $J$'s. The even and odd $J$ components of these bands will have slightly different molecular constants due to the $l$ doubling.

Spectra with Doppler-limited resolution were obtained using current-tuned, PbTe diode lasers. Lower resolution spectra taken at different temperatures were obtained with a Fourier transform spectrometer, and these aided in the identification and analysis of the ground state transitions. The molecular constants $B$, $D$, and $H$ were obtained for each band identified using a least squares computer fit to the standard polynomial expansion in $J$ appropriate for a linear molecule. Our results agree with those of Mantz *et al.*[17] for the ground and $2\nu_7^0$ states and with assignment 2 of Lafferty *et al.*[16] for the $\nu_7^1$ state. The $D$ terms were found to be anomalously large compared with other similar molecules, suggesting that the primary effect of centrifugal distortion is a reduction in amplitude of the bending mode $\nu_7$.

## II. EXPERIMENTAL

### A. Diode lasers

The diode lasers were made from single crystal PbTe epitaxial films typically 4 μ thick grown on $BaF_2$

  

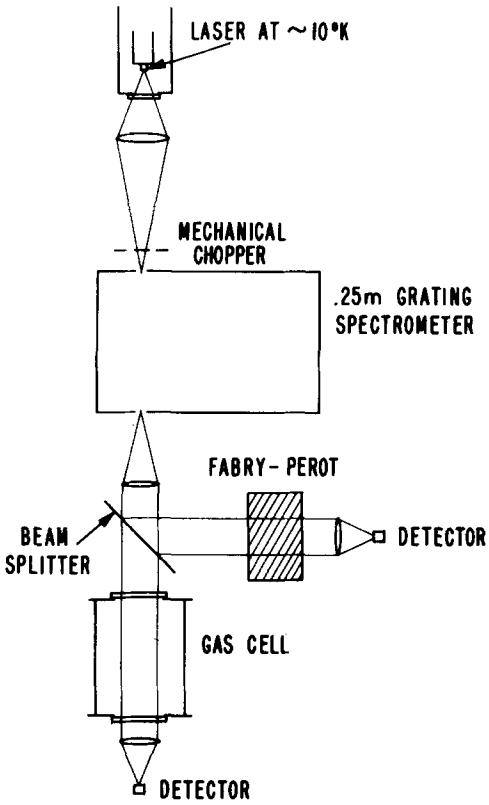


FIG. 1. Experimental arrangement for diode laser spectroscopy. The beam splitter is a thin silicon wafer, the Fabry–Perot is a 4-cm Ge etalon, the detectors are liquid-nitrogen-cooled Ge : Au photoconductors, and the windows and lenses are $BaF_2$.

substrates. The laser cavities were 200 to 400 $\mu$ long. End facets were produced by photoresist etching. An evaporated Pb film electrode provided the minority carrier injection required for lasing. Continuous wave lasing was obtained at diode temperatures below about 20 K. The properties of these devices and details of their fabrication have been described previously.[6,18] Tuning was accomplished by varying the current (50–250 mA) through the diode. The joule heating by the diode current produced a change of the temperature and consequently of the refractive index in the active PbTe region, leading to a change in the laser frequency. The continuous tuning range of a single mode was typically 1.5 to 2 $cm^{-1}$, which is somewhat larger than that normally obtained with bulk crystal Pb–salt lasers.[1,5,19] Without this broader tuning range the identification of the various series of lines, whose spacings were typically 0.3 $cm^{-1}$, would have been very difficult. Normally 2–3 modes lase simultaneously in a particular diode and the frequencies of these modes shift somewhat when the Dewar is recycled from room temperature to liquid He temperature on different days. In addition, these diodes do not have a simple mode pattern, but tend to lase in two distinct regions some 10 to 15 $cm^{-1}$ apart. The positions and separations of these two regions vary from diode to diode.

By using all the available modes of three different lasers, roughly 70% of a 35 $cm^{-1}$ region extending from 1565 to 1600 $cm^{-1}$ has been covered. There are five gaps remaining in the spectrum, the largest being 5 $cm^{-1}$ centered at 1595 $cm^{-1}$, while the other four are on the order of 1 $cm^{-1}$.

### B. Calibration

A diagram of the apparatus is shown in Fig. 1. The 25 cm focal length grating spectrometer is used to select individual modes and to provide rough calibration. Relative frequency calibration is obtained from the fringes of a 4-cm thick uncoated Ge étalon, recorded simultaneoulsy with the absorption spectrum using a double beam technique. The fringe separation was calculated at 5 $cm^{-1}$ intervals using the measured thickness and the published refractive index values, including dispersion.[20] This quantitiy varied smoothly from 0.032770 $cm^{-1}$ at 1565 $cm^{-1}$ to 0.032759 $cm^{-1}$ at 1600 $cm^{-1}$. From analysis of multiple records of the same spectral regions we found the rms uncertainty associated with measuring the separation between two strong lines to vary from about $\pm 0.0005$ $cm^{-1}$ to 0.002 $cm^{-1}$, depending on the signal-to-noise ratio in the fringe and signal channels.

The double beam technique greatly improves the accuracy with which frequency differences can be measured. Although the frequency of a laser mode increases monotonically with the diode current, it has a nonlinear dependence on this quantity. In addition, there are temperature fluctuations in the Dewar which produce small but random changes in the laser frequency. Both of these difficulties preclude using the diode current to accurately monitor the laser frequency. Also, any disruption of the uniform progression of fringes served to indicate a changed laser mode structure and possible leakage of a second mode through the spectrometer.

Absolute calibration is obtained with $H_2O$ and $NH_3$ lines.[21,22] Since there is some arbitrariness in the choice of reference lines, we show in Table I a summary of the calibration points used in the various spectral regions. The separations of several closely

TABLE I. Summary of calibration lines used in various spectral regions. Line positions are taken from Refs. 21 and 22.

| Spectral region ($cm^{-1}$) | Calibration |
|---|---|
| 1597–1600 | $NH_3$ line # 349 at 1599.0696 $cm^{-1}$. |
| 1590–1592 | Average of $a^PP(2,1)$ and $s^PP(2,1)$ $NH_3$ lines at 1590.8844 $cm^{-1}$. |
| 1583–1589 | $a^RP(2,0)$ $NH_3$ line at 1586.8593 $cm^{-1}$ |
| 1576–1581 | Linear interpolation between the average of the $a^PP(3,3)$ and $s^PP(3,3)$ $NH_3$ lines at 1579.4838 $cm^{-1}$ and the $5_{3,2}-6_{2,5}$ $H_2O$ line at 1577.5839 $cm^{-1}$. |
| 1572–1576 | Linear interpolation between the $s^PP(3,2)$ $NH_3$ line at 1575.8520 $cm^{-1}$ and the $a^PP(3,1)$ $NH_3$ line at 1572.4827 $cm^{-1}$. |
| 1565–1569 | $s^RP(3,0)$ $NH_3$ line at 1567.9901 $cm^{-1}$. |

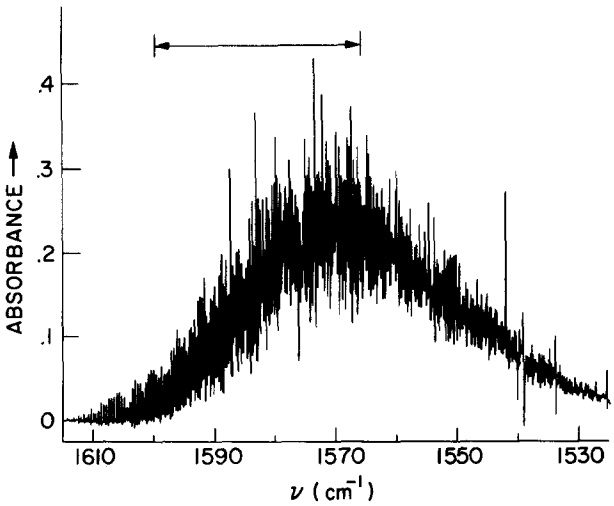


FIG. 2. Room temperature Fourier transform spectrum at 5 torr and 0.5 m path length in the $\nu_4$ band of $^{12}C_3\,^{16}O_2$. The curve was obtained by straight line interpolation of digitized absorbance values computed at $\frac{1}{16}$ $cm^{-1}$ intervals. The arrows indicate the range of the laser data. Most of the large spikes can be attributed to interference from strong (~100% absorbing) $H_2O$ lines which produced large errors in the ratioed absorbance data, e.g., the apparent dips at 1576 and 1539 $cm^{-1}$ and the spikes at 1542 and 1534 $cm^{-1}$.

spaced $NH_3$ inversion doublets measured with our apparatus agreed (±0.001 $cm^{-1}$) with the recent microwave results of Cohen and Poynter,[23] but they were systematically smaller (~0.02 $cm^{-1}$) than the reported infrared values.[22] To compensate for these errors, apparently associated with deconvoluting the incompletely resolved grating spectra, we used the mean values of the inversion pairs for calibration.

In two spectral regions, each involving several overlapping charts, we determined the fringe spacing for calibration by measuring the separations of two widely spaced $H_2O$ or $NH_3$ lines near the ends of the regions. This procedure was necessary since the endpoint calibration line separations measured in terms of the calculated fringe spacing differed from the reported separations by a few parts per thousand in both spectral regions. At the moment we attribute these discrepancies to either or both or two possibilities: the index and dispersion of our Ge étalon differ from the published values, and/or there are small errors (~$10^{-2}$ $cm^{-1}$) in some of the reported line positions.

### C. Sample preparation

Carbon suboxide samples were obtained by the decomposition of malonic acid in a mixture of dry sand and phosphorus pentoxide. This mixture was heated in vacuum to 140°C and the reaction products collected in a liquid nitrogen trap. Fractional distillation was then used to obtain a pure liquid sample of $C_3O_2$. This concentrated sample could be kept at 77 K indefinitely. Gas samples at 10 torr were kept for several months at −20°C with no sign of decomposition. The above procedure has been demonstrated to yield high purity $C_3O_2$ samples.[13] The only impurity identified from the infrared spectra was a trace amount of $CO_2$.

## III. RESULTS

### A. Fourier transform spectra

A Fourier transform spectrum of the $\nu_4$ band of $C_3O_2$ is shown in Fig. 2 at a resolution of 0.063 $cm^{-1}$. These data were obtained with an Eocom Corp. model 7001 laser-controlled, scanning Michelson interferometer and a Digital Equipment Corp. PDP 11/40 computer. This instrument has been described previously[24] and will be described in more detail in a subsequent publication. The arrows at the top of Fig. 2 indicate the range of the laser data. The only resolvable series in this spectrum is the set of strong, single-channel lines which stand out above 1600 $cm^{-1}$. This series is the *R* branch of the ground state transition. The absence of correspondingly strong lines on the low frequency side of the band indicates a greater density of weaker lines in that region. This suggests that the hot bands are shifted to lower frequencies relative to the ground state transitions.

Figure 3 shows a Fourier transform spectrum of the difference between the absorbance at room temperature and 193 K. The cell pressure was 5 torr, which was low enough to prevent condensation upon cooling. The resolution is 0.63 $cm^{-1}$ and all of the sharp structure observed is due to atmospheric $H_2O$ interference. The increase in the room temperature absorbance on the low frequency side of the band is a further indication that the hot bands are progressively displaced to lower frequencies. This is opposite to the behavior of the hot bands in the combination band first studied by Lafferty *et al.*[16] and later identified as $2\nu_2+\nu_4$ by Mantz *et al.*[17]

### B. Laser spectra

Laser spectra were recorded at low pressures (0.05–0.5 torr) to eliminate pressure broadening. The resolution under these conditions should be limited

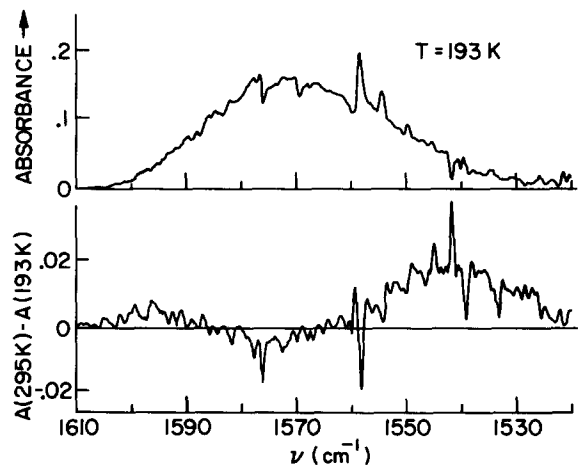


FIG. 3. The upper trace is a Fourier transform spectrum at 193 K of $C_3O_2$ at 5 torr and 0.5 m path length with 10 channels averaged together (0.63 $cm^{-1}$ resolution) to remove the rotational structure. The lower trace is the difference between the room temperature and 193 K absorbance curves on the same sample. Most of the sharp structure is due to $H_2O$ interference.

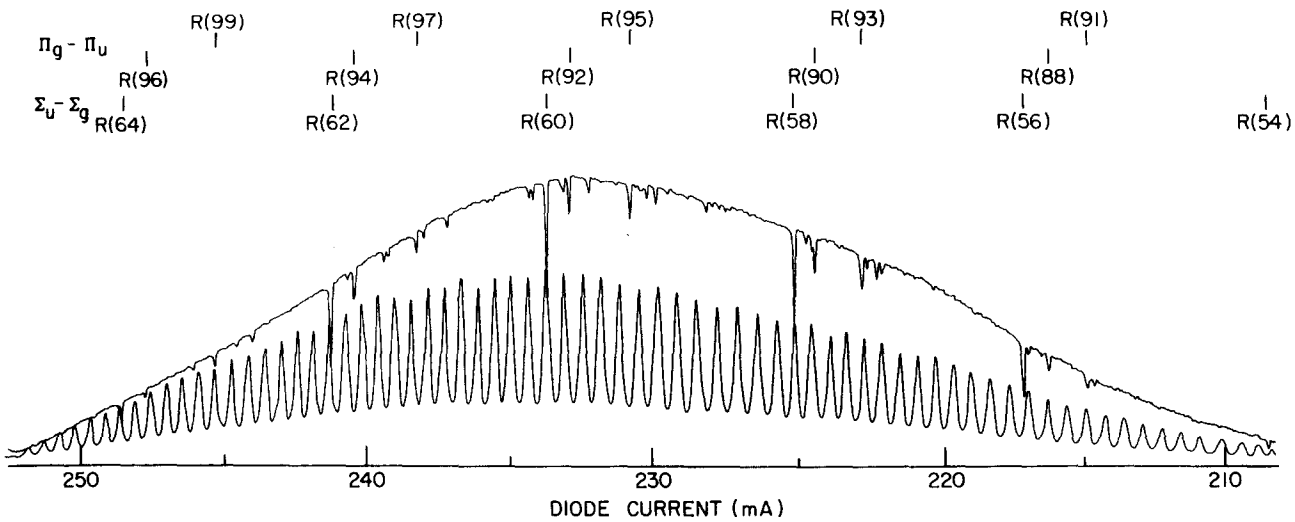


FIG. 4. A 2.3 $cm^{-1}$ long diode laser spectrum of $C_3O_2$ at 0.1 torr and 3.2 m path length. The spectral region is 1597–1600 $cm^{-1}$ and the calculated fringe spacing is 0.032759 $cm^{-1}$. The assignment of the odd-$J$ $\Pi$–$\Pi$ series is tentative; it differs by 2 from that indicated in Table III.

by the laser linewidth $\Delta\nu_L$ and the natural Doppler width $\Delta\nu_D$ given by

$$\Delta\nu_D(\mathrm{cm}^{-1}) = 7.17\times10^{-7}\,\nu(T/M)^{1/2} \approx 0.0024\ \mathrm{cm}^{-1}.$$

Although we have not attempted to measure $\Delta\nu_L$ directly, comparisons of the observed absorption linewidths with $\Delta\nu_D$ above indicate $\Delta\nu_L \lesssim 10^{-3}$ $cm^{-1}$. This result is consistent with the theoretical estimate $\Delta\nu_L \approx 10^{-4}$ $cm^{-1}$ for a typical laser mode emitting a few $\mu$W of power.[1]

Figure 4 shows a 2.3 $cm^{-1}$ laser scan at the highest frequency obtained with our lasers. The strongest lines in this figure are the same resolved lines appearing near 1600 $cm^{-1}$ in Fig. 2, and we have identified these as the $R$ branch of the ground state transition. Since we expect the hot bands to be systematically shifted to lower frequencies, we would identify the next strongest series of lines, of which there are two with about equal intensities, to be the even and odd $J$ components of the $l$-doubled $\Pi$–$\Pi$ series associated with $\nu_7^1$ in the lower state.

A laser scan 1.7 $cm^{-1}$ long near the band origin of the ground state transition is shown in Fig. 5. The first few $R$-branch lines for this series are indicated. An overlapping scan at lower frequencies shows the beginning of the $P$ branch for the same series. The relative intensities of the small $J$ lines and the gap between $R(0)$ and $P(2)$ of 1.5 times the normal spacing established the position of the band origin. This is the only band in which we have identified unambiguously all the lines on either side of the band origin. The determinations of band origins for the other series generally required trial and error fits to various possibilities, since the large density of weak lines occurring at lower frequencies usually made positive identification of the

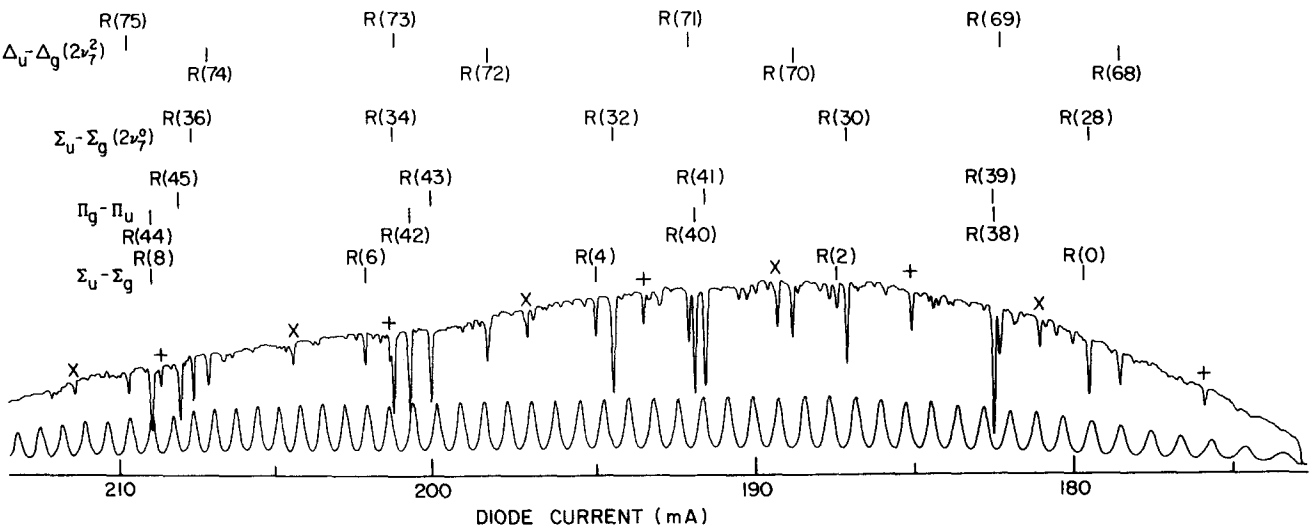


FIG. 5. A 1.7 $cm^{-1}$ long diode laser spectrum of $C_3O_2$ at 0.1 torr and 3.2 m path length. The spectral region is 1587–1589 $cm^{-1}$ and the calculated fringe spacing is 0.032762 $cm^{-1}$. The ground state $R(0)$ line appears as a weak shoulder on the high frequency side of the $2\nu_7^0$ $R(28)$ line.

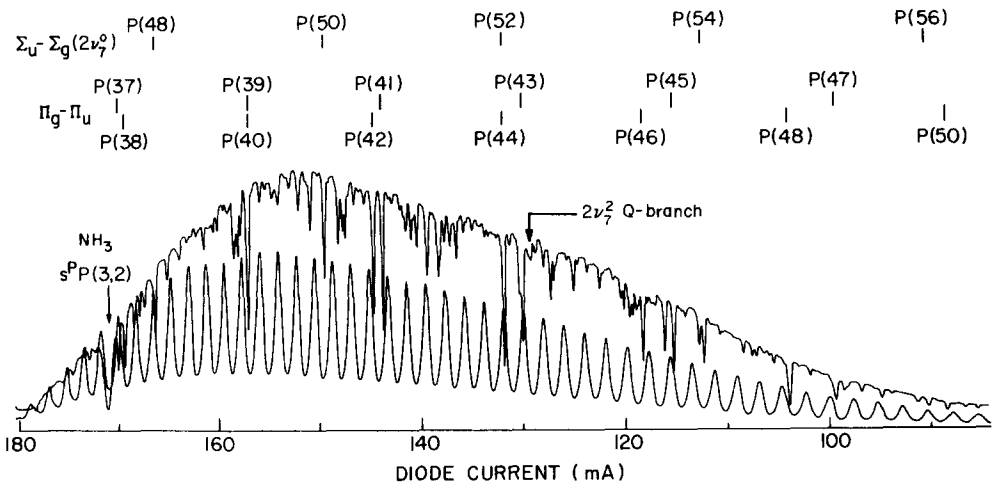


FIG. 6. A 1.6 $cm^{-1}$ long diode laser spectrum of $C_3O_2$ at 0.1 torr and 3.2 m path length. The $NH_3$ $s^PP(3,2)$ line is at 1575.8520 $cm^{-1}$ and the calculated fringe spacing is 0.032767 $cm^{-1}$. The $NH_3$ at several torr pressure is contained in a separate 10 cm cell in series with the $C_3O_2$ cell.

first few $J$ lines impossible.

There are several other series apparent in Fig. 5, besides the extensions of the three already identified in Fig. 4. The strongest of these is a $\Sigma-\Sigma$ band, and we have assigned it to a transition whose lower vibrational state is $2\nu_7^0$. Next in strength are two series, of about equal intensity and spacing, which are displaced from each other by nearly half the line spacing. We have identified these series as a $\Delta-\Delta$ band associated with $2\nu_7^2$ in the lower state. This assignment is consistent with the expected systematic shift of the hot bands to lower $\nu$ and the expected small value for the $l$-doubling constant. The $l$-doubling constant should be extremely small in a $\Delta-\Delta$ band, thus the two series will appear to be a single series with half the line spacing until quite large $J$ values are reached.

There still remain two identifiable series in Fig. 5, which are marked with the + and × symbols. These have roughly equal intensities with slightly different spacings. The assignment of these series is quite tentative, since we have been unable to identify the corresponding $P$ branches. However, the most logical choices are a $\Pi-\Pi$ or a $\Phi-\Phi$ band, associated with $3\nu_7^1$ or $3\nu_7^3$, respectively. We presently favor the $3\nu_7^1$ assignment, since the $l$-doubling constant appears to be too large for the $l=3$ state.

Figure 6 shows a 1.5 $cm^{-1}$ scan near the region of maximum average absorption. The $P$-branch lines for several of the series appearing in Fig. 5 are shown in this figure, as well as the $NH_3$ $s^PP(3,2)$ line at 1575.8520 $cm^{-1}$ used for calibration. The diode current scale is linear, and a marked decrease in the fringe spacing is observed at high currents, indicative of the nonlinear dependence of the laser frequency on diode current. Due to the large density of weak lines we were able to identify only the strongest series in this spectral region and at lower frequencies. Even for these strong series, overlapping was often a problem. Note, for example, that both the $P(40)$ and $P(44)$ $\Pi_g-\Pi_u$ lines in Fig. 6 are overlapped.

Also shown in Fig. 6 is our tentative assignment of the $2\nu_7^2$ $Q$ branch. Weak $Q$ branches are allowed for the $l\neq 0$ states, but assigning them is very difficult since the lines decrease in intensity as $J$ increases, the strongest being only 15% of the intensity of the strongest $P$- or $R$-branch lines.[25] The assignment in Fig. 6 was achieved only after the corresponding $P$ and $R$ branches had been found. The individual lines are not resolved but the shape, position, and intensity of the band are consistent with the $Q$-branch assignment.

## IV. BAND ANALYSES AND MOLECULAR CONSTANTS

The molecular constants for each band were determined by fitting the observed line positions to the usual polynomial expansion in $m$:

$$\nu = \nu_0 + (B'+B'')m + (B'-B'')m^2 - 2(D'+D'')m^3 - (D'-D'')m^4 + 3(H'+H'')m^5 + (H'-H'')m^6, \quad (1)$$

where $m=-J$ for the $P$ branch and $m=J+1$ for the $R$ branch. Approximate values for the molecular constants were obtained first by graphical methods using combination sums and differences. These values were then refined by a least-squares computer program. Since the gaps in the spectrum often limited the sums and differences to about half of the $J$ values, the accuracy of the constants was greatly improved by the computer fit, which used all the observed lines.

### A. $\Sigma_u-\Sigma_g$ ground state

Table II gives the observed frequencies and the errors between the observed and calculated frequencies for the transitions originating in the ground vibrational state. Data for lines above 1600 $cm^{-1}$ were taken from the Fourier transform spectra. These lines have a statistical uncertainty of approximately ±0.02 $cm^{-1}$, i.e., at least an order of magnitude greater than those measured with the lasers. Absolute calibration of the Fourier transform data was adjusted to agree with the same $NH_3$ lines used for calibrating the laser data.

The intensities measured with the Fourier transform spectrometer of the individual $R$ lines near $J=60$ were found to increase 10%–20% when the sample was cooled to 193 K. This intensity change is consistent with the ground state assignment, since the rotational Boltzmann factor alone would predict a sizable decrease in intensity.

TABLE II. Observed frequencies (vac. $cm^{-1}$) of $\nu_4$ $1 \leftarrow 0$ ground state transitions. Lines above 1600 $cm^{-1}$ are determined from the Fourier transform spectrometer data. The rms error of the fit using the molecular constants in Table VIII is $\pm 0.0021$ $cm^{-1}$ for the 58 lines below 1600 $cm^{-1}$ and $\pm 0.0071$ $cm^{-1}$ for all 82 lines.

| $J$ | $R(J)$ OBS | O–C | $P(J)$OBS | O–C |
|---|---|---|---|---|
| 0 | 1587.5398 | −0.0028 | ... | ... |
| 2 | 1587.8506 | −0.0008 | 1587.0887 | −0.0005 |
| 4 | 1588.1645 | −0.0007 | 1586.7898 | −0.0036 |
| 6 | 1588.4835 | −0.0007 | 1586.4999 | −0.0028 |
| 8 | 1588.8103 | 0.0020 | 1586.2188 | 0.0016 |
| 10 | 1589.1381 | 0.0007 | 1585.9376 | 0.0008 |
| 12 | ... | ... | 1585.6623 | 0.0008 |
| 14 | ... | ... | 1585.3913 | −0.0001 |
| 16 | ... | ... | 1585.1267 | 0.0005 |
| 18 | 1590.4989 | −0.0043 | 1584.8672 | 0.0011 |
| 20 | 1590.8551 | −0.0016 | 1584.6129 | 0.0020 |
| 22 | 1591.2153 | 0.0005 | 1584.3612 | 0.0006 |
| 24 | 1591.5797 | 0.0022 | 1584.1180 | 0.0028 |
| 26 | 1591.9488 | 0.0042 | 1583.8766 | 0.0021 |
| 28 | 1592.3216 | 0.0054 | 1583.6396 | 0.0012 |
| 30 | ... | ... | 1583.4080 | 0.0011 |
| 54 | 1597.4861 | −0.0006 | ... | ... |
| 56 | 1597.9042 | −0.0013 | 1580.7629 | 0.0002 |
| 58 | 1598.3238 | −0.0026 | 1580.5812 | −0.0013 |
| 60 | 1598.7477 | −0.0017 | 1580.4034 | −0.0015 |
| 62 | 1599.1708 | −0.0034 | 1580.2269 | −0.0027 |
| 64 | 1599.5951 | −0.0055 | 1580.0529 | −0.0036 |
| 66 | 1600.0300 | 0.0016 | 1579.8835 | −0.0019 |
| 68 | 1600.4520 | −0.0054 | 1579.7149 | −0.0012 |
| 70 | 1600.8740 | −0.0136 | 1579.5482 | −0.0001 |
| 72 | 1601.2960 | −0.0225 | 1579.3796 | −0.0024 |
| 74 | 1601.7780 | 0.0279 | 1579.2168 | −0.0001 |
| 76 | 1602.2000 | 0.0178 | 1579.0519 | −0.0009 |
| 78 | 1602.6220 | 0.0075 | 1578.8897 | 0.0003 |
| 80 | 1603.0440 | −0.0029 | 1578.7277 | 0.0010 |
| 82 | 1603.4660 | −0.0132 | 1578.5664 | 0.0020 |
| 84 | ... | ... | 1578.4046 | 0.0023 |
| 86 | ... | ... | 1578.2418 | 0.0016 |
| 88 | 1604.7910 | 0.0179 | 1578.0790 | 0.0012 |
| 90 | 1605.2130 | 0.0102 | 1577.9161 | 0.0010 |
| 92 | 1605.6450 | 0.0136 | 1577.7535 | 0.0018 |
| 94 | 1606.0570 | −0.0017 | 1577.5910 | 0.0036 |
| 96 | 1606.4790 | −0.0055 | 1577.4230 | 0.0009 |
| 98 | 1606.9010 | −0.0077 | 1577.2549 | −0.0007 |
| 100 | 1607.3220 | −0.0090 | 1577.0852 | −0.0024 |
| 102 | 1607.7440 | −0.0072 | 1576.9154 | −0.0026 |
| 104 | 1608.1660 | −0.0032 | 1576.7457 | −0.0009 |
| 106 | 1608.5880 | 0.0031 | ... | ... |
| 108 | 1609.0100 | 0.0120 | ... | ... |
| 112 | 1609.7930 | −0.0231 | ... | ... |
| 114 | 1610.2150 | −0.0058 | ... | ... |
| 116 | 1610.6370 | 0.0146 | ... | ... |
| 120 | 1611.4200 | 0.0043 | ... | ... |

### B. $\Pi_g - \Pi_u$ $\nu_4 + \nu_7^1 \leftarrow \nu_7^1$

The observed frequencies of the $\Pi-\Pi$ bands are shown in Tables III and IV. The $J$ assignment of the $R(J \geq 89)$ lines in Table III is tentative, since these lines appear to be strongly perturbed. An alternative assignment, based only on the extrapolation back to the $R(53-63)$ region, is used to label this series in Fig. 4. Neither assignment gives a reasonable fit to Eq. (1), and for this reason we have omitted these lines from the determination of molecular constants. A Coriolis interaction is probably the source of the perturbation of these lines. Two possible vibrations which have both the correct symmetry and approximately the right frequency for a Coriolis interaction with $\nu_4 + \nu_7^1$ are $2\nu_2$ and $3\nu_6^1 + \nu_7^1$. There is no evidence of perturbations in the even $-J$ $\Pi-\Pi$ band given in Table IV, and all the lines are included in the fit for that band.

### C. $\Delta_u - \Delta_g$ $\upsilon_4 + 2\nu_7^2 \leftarrow 2\nu_7^2$

The observed frequencies for the $\Delta-\Delta$ bands are shown in Tables V and VI. The weak Coriolis perturbation apparent in the $R(61)$ and $P(63)$ lines of the odd $-J$ series in Table V allowed us to assign these two series with some certainty. Without relying on the fact that the perturbed levels have a common upper state, other possible assignments for the band origin

TABLE III. Observed frequencies (vac. $cm^{-1}$) of the $\nu_4 + \nu_7^{1c} \leftarrow \nu_7^{1c}$ transitions. The $J \geq 80$ $R$ lines appear to be highly perturbed and are not included in the computer fit. Even the assignment of $J$ values for these lines is tentative, since the extrapolation to lower $J$ did not yield an unambiguous assignment. The rms error of the fit using the molecular constants in Table VIII is $\pm 0.0023$ $cm^{-1}$ for 57 lines.

| $J$ | $R(J)$ OBS | O–C | $P(J)$OBS | O–C |
|---|---|---|---|---|
| 5 | ... | ... | 1580.1428 | −0.0020 |
| 7 | ... | ... | 1579.8485 | −0.0019 |
| 9 | ... | ... | 1579.5579 | −0.0017 |
| 11 | ... | ... | 1579.2699 | −0.0024 |
| 13 | ... | ... | 1578.9885 | −0.0001 |
| 15 | 1583.4499 | 0.0012 | 1578.7103 | 0.0020 |
| 17 | 1583.7844 | 0.0016 | 1578.4348 | 0.0033 |
| 19 | 1584.1202 | 0.0001 | 1578.1609 | 0.0028 |
| 21 | 1584.4615 | 0.0010 | 1577.8918 | 0.0037 |
| 23 | 1584.8035 | −0.0004 | 1577.6253 | 0.0040 |
| 25 | 1585.1488 | −0.0014 | 1577.3609 | 0.0031 |
| 27 | 1585.4974 | −0.0020 | 1577.0982 | 0.0008 |
| 29 | 1585.8506 | −0.0008 | 1576.8396 | −0.0005 |
| 31 | 1586.2101 | 0.0040 | 1576.5833 | −0.0024 |
| 33 | 1586.5644 | 0.0009 | ... | ... |
| 35 | 1586.9205 | −0.0030 | 1576.0817 | −0.0040 |
| 37 | 1587.2835 | −0.0025 | 1575.8350 | −0.0049 |
| 39 | 1587.6496 | −0.0014 | 1575.5925 | −0.0042 |
| 41 | 1588.0176 | −0.0009 | 1575.3512 | −0.0048 |
| 43 | 1588.3887 | 0.0003 | 1575.1148 | −0.0031 |
| 45 | 1588.7618 | 0.0012 | 1574.8804 | −0.0018 |
| 47 | 1589.1381 | 0.0028 | 1574.6489 | 0.0001 |
| 49 | ... | ... | 1574.4211 | 0.0035 |
| 51 | ... | ... | 1574.1918 | 0.0031 |
| 53 | 1590.2728 | −0.0009 | 1573.9631 | 0.0012 |
| 55 | 1590.6591 | 0.0010 | 1573.7394 | 0.0022 |
| 57 | 1591.0470 | 0.0018 | 1573.5159 | 0.0014 |
| 59 | 1591.4366 | 0.0016 | 1573.2967 | 0.0027 |
| 61 | 1591.8274 | −0.0003 | 1573.0754 | −0.0000 |
| 63 | 1592.2204 | −0.0031 | 1572.8615 | 0.0025 |
| 65 | ... | ... | 1572.6447 | 0.0001 |
| 67 | ... | ... | 1572.4325 | 0.0000 |
| 69 | ... | ... | 1572.2206 | −0.0019 |
| 71 | ... | ... | 1572.0140 | −0.0010 |
| 73 | ... | ... | 1571.8087 | −0.0012 |
| 89 | 1597.7941 | 0.0002 | ... | ... |
| 91 | 1598.1957 | −0.0775 | ... | ... |
| 93 | 1598.6002 | −0.1633 | ... | ... |
| 95 | 1599.0017 | −0.2641 | ... | ... |
| 97 | 1599.4036 | −0.3776 | ... | ... |

TABLE IV. Observed frequencies (vac. $cm^{-1}$) of the $\nu_4+\nu_7^{1d}\leftarrow\nu_7^{1d}$ transitions. The rms error of the fit using the molecular constants in Table VIII is $\pm 0.0031$ $cm^{-1}$ for 63 lines.

| $J$ | $R(J)$ OBS | O–C | $P(J)$ OBS | O–C |
|---|---|---|---|---|
| 6 | ... | ... | 1579.9931 | −0.0072 |
| 8 | ... | ... | 1579.7000 | −0.0086 |
| 10 | ... | ... | 1579.4144 | −0.0067 |
| 12 | ... | ... | 1579.1347 | −0.0031 |
| 14 | 1583.3254 | 0.0048 | 1578.8588 | −0.0000 |
| 16 | 1583.6633 | 0.0025 | 1578.5831 | −0.0009 |
| 18 | 1584.0080 | 0.0030 | 1578.3140 | 0.0007 |
| 20 | 1584.3556 | 0.0025 | 1578.0477 | 0.0010 |
| 22 | 1584.7083 | 0.0032 | 1577.7875 | 0.0033 |
| 24 | 1585.0644 | 0.0035 | 1577.5288 | 0.0031 |
| 26 | 1585.4234 | 0.0029 | 1577.2744 | 0.0032 |
| 28 | 1585.7871 | 0.0034 | 1577.0218 | 0.0012 |
| 30 | 1586.1562 | 0.0057 | 1576.7737 | −0.0000 |
| 32 | 1586.5213 | 0.0006 | 1576.5304 | −0.0003 |
| 34 | 1586.8915 | −0.0029 | ... | ... |
| 36 | 1587.2685 | −0.0029 | 1576.0570 | 0.0015 |
| 38 | 1587.6491 | −0.0025 | 1575.8213 | −0.0019 |
| 40 | 1588.0312 | −0.0037 | 1575.5928 | −0.0015 |
| 42 | 1588.4176 | −0.0035 | 1575.3675 | −0.0012 |
| 44 | 1588.8079 | −0.0024 | 1575.1456 | −0.0008 |
| 46 | 1589.2020 | −0.0002 | 1574.9275 | 0.0004 |
| 48 | ... | ... | 1574.7172 | 0.0064 |
| 50 | ... | ... | 1574.5008 | 0.0033 |
| 52 | 1590.3889 | −0.0046 | 1574.2890 | 0.0021 |
| 54 | 1590.7923 | −0.0031 | 1574.0801 | 0.0012 |
| 56 | 1591.1989 | −0.0005 | 1573.8751 | 0.0016 |
| 58 | 1591.6074 | 0.0019 | 1573.6704 | −0.0001 |
| 60 | 1592.0176 | 0.0040 | 1573.4678 | −0.0020 |
| 62 | ... | ... | 1573.2692 | −0.0020 |
| 64 | ... | ... | 1573.0729 | −0.0018 |
| 66 | ... | ... | 1572.8775 | −0.0025 |
| 68 | ... | ... | 1572.6845 | −0.0026 |
| 70 | ... | ... | 1572.4956 | −0.0003 |
| 72 | ... | ... | 1572.3028 | −0.0033 |
| 74 | ... | ... | 1572.1161 | −0.0016 |
| 76 | ... | ... | 1571.9316 | 0.0011 |
| 78 | ... | ... | 1571.7503 | 0.0058 |
| 88 | 1597.8626 | 0.0026 | ... | ... |
| 90 | 1598.2854 | 0.0028 | ... | ... |
| 92 | 1598.7065 | 0.0012 | ... | ... |
| 94 | 1599.1271 | −0.0010 | ... | ... |
| 96 | 1599.5473 | −0.0035 | ... | ... |

would have to be considered. As in the case of the Π–Π bands, there are at least two vibrational states which might be causing a Coriolis perturbation in the Δ–Δ bands: $2\nu_2+\nu_7^1$ or $3\nu_6^1+2\nu_7^0$.

### D. $\Sigma_u-\Sigma_g$ $\nu_4+2\nu_7^0\leftarrow 2\nu_7^0$

Table VII gives the observed frequencies for the transitions $\nu_4+2\nu_7^0\leftarrow 2\nu_7^0$. The band origin for this series was determined by trying several possible assignments and then choosing the one giving the best fit to Eq. (1). The intensity of the Σ–Σ $2\nu_7^0$ band is substantially below that of the Σ–Σ ground state band, and we can use this fact to obtain a rough estimate of the $2\nu_7^0$ vibrational energy. The line strengths of the $P(50)$ and $P(54)$ $2\nu_7^0$ lines, corrected for the expected $J$ dependence, were ≈70% of those for the similarly corrected $R(56)$–$R(62)$ ground state lines, recorded under identical conditions of pressure and scanning rate. If we make the admittedly weak assumption that the transition moments for the two sets of lines are the same, then the intensity difference is due solely to a vibrational Boltzmann factor, which leads to the estimate $73\pm 30$ $cm^{-1}$ for the $2\nu_7^0$ state. This range of values is consistent with the value 61 $cm^{-1}$ found by Carreira *et al.*[15] and Mantz *et al.*[17] The large uncertainty is due primarily to the uncertainty in line strengths caused by weak overlapping lines.

### E. Molecular constants

A summary of the molecular constants is given in Table VIII. The uncertainties quoted in the Table are rough estimates which include both the statistical uncertainty and some allowance for possible errors in the calibration points. The ground state contains the largest number of lines and the highest $J$ values and is the only band for which the $H$ terms are determined with any degree of accuracy. Our molecular constants for the ground state are in good agreement with those of Mantz *et al.*,[17] but the agreement in the $2\nu_7^0$ state is not quite as good—our values of $B''$ and $D''$ being somewhat larger. For the $\nu_7^1$ states our $B''$ values and the $l$-doubling constant $q_1''=B_d''-B_c''=3.6$ $(\pm 0.6)\times 10^{-4}$ $cm^{-1}$ support Assignment 2 proposed by Lafferty *et al.*[16] in their analysis of the Π–Π bands.

TABLE V. Observed frequencies (vac. $cm^{-1}$) of the $\nu_4+2\nu_7^{2c}\leftarrow 2\nu_7^{2c}$ transitions. The $J=62$ upper level appears to be perturbed and the two transitions associated with it are omitted from the fit. The rms error of the fit using the molecular constants in Table VIII is $\pm 0.0032$ $cm^{-1}$ for 48 lines.

| $J$ | $R(J)$ OBS | O–C | $P(J)$ OBS | O–C |
|---|---|---|---|---|
| 7 | ... | ... | 1574.0383 | 0.0046 |
| 9 | 1576.6750 | −0.0004 | 1573.7436 | 0.0057 |
| 11 | 1577.0010 | −0.0001 | 1573.4498 | 0.0044 |
| 13 | 1577.3346 | 0.0047 | 1573.1515 | −0.0046 |
| 15 | 1577.6648 | 0.0031 | 1572.8709 | 0.0010 |
| 17 | 1577.9992 | 0.0026 | 1572.5842 | −0.0027 |
| 19 | 1578.3372 | 0.0027 | 1572.3031 | −0.0040 |
| 21 | ... | ... | 1572.0250 | −0.0055 |
| 23 | 1579.0156 | −0.0038 | 1571.7505 | −0.0065 |
| 25 | 1579.3609 | −0.0053 | ... | ... |
| 27 | ... | ... | ... | ... |
| 31 | 1580.4181 | −0.0059 | ... | ... |
| 33 | 1580.7784 | −0.0038 | ... | ... |
| 45 | ... | ... | 1568.9518 | 0.0022 |
| 47 | 1583.3649 | 0.0005 | 1568.7141 | 0.0024 |
| 49 | 1583.7433 | 0.0001 | 1568.4803 | 0.0038 |
| 51 | 1584.1256 | 0.0012 | 1568.2475 | 0.0037 |
| 53 | 1584.5089 | 0.0012 | 1568.0150 | 0.0014 |
| 55 | 1584.8948 | 0.0016 | 1567.7870 | 0.0012 |
| 57 | 1585.2850 | 0.0042 | 1567.5608 | 0.0004 |
| 59 | 1585.6748 | 0.0045 | 1567.3362 | −0.0010 |
| 61 | 1586.0740 | 0.0124 | 1567.1139 | −0.0022 |
| 63 | 1586.4531 | −0.0016 | 1566.9019 | 0.0049 |
| 65 | 1586.8493 | −0.0002 | 1566.6743 | −0.0055 |
| 67 | 1587.2436 | −0.0021 | 1566.4613 | −0.0030 |
| 69 | 1587.6414 | −0.0020 | 1566.2498 | −0.0006 |
| 71 | 1588.0404 | −0.0019 | 1566.0391 | 0.0011 |
| 73 | 1588.4409 | −0.0014 | 1565.8299 | 0.0031 |
| 75 | 1588.8428 | −0.0005 | ... | ... |
| 77 | 1589.2479 | 0.0028 | ... | ... |

TABLE VI. Observed frequencies (vac. $cm^{-1}$) of the $\nu_4+2\nu_7^{2d} \leftarrow 2\nu_7^{2d}$ transitions. The rms error of the fit using the molecular constants in Table VIII is $\pm 0.0038$ $cm^{-1}$ for 50 lines.

| $J$ | $R(J)$ OBS | O−C | $P(J)$ OBS | O−C |
|---|---|---|---|---|
| 8 | ... | ... | 1573.8920 | 0.0084 |
| 10 | ... | ... | 1573.5939 | 0.0044 |
| 12 | 1577.1705 | 0.0076 | 1573.2948 | −0.0039 |
| 14 | 1577.4988 | 0.0055 | 1573.0106 | −0.0005 |
| 16 | 1577.8293 | 0.0025 | 1572.7250 | −0.0017 |
| 18 | 1578.1646 | 0.0013 | 1572.4430 | −0.0025 |
| 20 | 1578.5037 | 0.0007 | 1572.1630 | −0.0046 |
| 22 | 1578.8442 | −0.0016 | 1571.8889 | −0.0041 |
| 24 | 1579.1895 | −0.0021 | ... | ... |
| 26 | 1579.5330 | −0.0075 | ... | ... |
| 28 | 1579.8881 | −0.0044 | ... | ... |
| 30 | 1580.2417 | −0.0058 | ... | ... |
| 32 | 1580.5999 | −0.0056 | ... | ... |
| 44 | ... | ... | 1569.0899 | 0.0044 |
| 46 | ... | ... | 1568.8528 | 0.0036 |
| 48 | 1583.5780 | 0.0035 | 1568.6160 | 0.0001 |
| 50 | 1583.9622 | 0.0041 | 1568.3870 | 0.0016 |
| 52 | 1584.3477 | 0.0035 | 1568.1571 | −0.0007 |
| 54 | 1584.7357 | 0.0030 | 1567.9323 | −0.0006 |
| 56 | 1585.1266 | 0.0031 | 1567.7050 | −0.0057 |
| 58 | 1585.5181 | 0.0015 | 1567.4910 | 0.0001 |
| 60 | 1585.9138 | 0.0020 | 1567.2726 | −0.0009 |
| 62 | 1586.3086 | −0.0003 | 1567.0556 | −0.0026 |
| 64 | 1586.7050 | −0.0028 | 1566.8432 | −0.0019 |
| 66 | 1587.1064 | −0.0018 | 1566.6341 | 0.0004 |
| 68 | 1587.5033 | −0.0068 | 1566.4291 | 0.0051 |
| 70 | 1587.9094 | −0.0038 | 1566.2201 | 0.0044 |
| 72 | 1588.3148 | −0.0025 | 1566.0102 | 0.0016 |
| 74 | 1588.7231 | 0.0011 | 1565.7968 | −0.0055 |
| 76 | 1589.1335 | 0.0064 | ... | ... |

## V. DISCUSSION

Although the structure of the $C_3O_2$ molecule is unquestionably linear, the very low frequency of $\nu_7$ will lead to a mean-squared structure that has significant bending. This bending can have an important influence on the molecular constants, an influence which becomes evident when we compare the data in Table VIII with results on other similar molecules and with results of electron diffraction measurements on $C_3O_2$.

The rotational constant $B$ for $C_3O_2$ can be calculated from

$$B=\frac{\hbar}{8\pi c}\,\frac{1}{m_O r_O^2+m_C r_C^2}\,, \tag{2}$$

where $r_O$ and $r_C$ are the distances from the rotational axis to the oxygen and carbon atoms, respectively; $m_O$ and $m_C$ are the corresponding masses. Recently Almenningen *et al.*[26,27] have measured by electron diffraction each of the atomic separations in $C_3O_2$. Using their values at 237 K of $r_O=2.3863$ Å, half of the O−O distance, and $r_C=1.2567$ Å, half of the larger C−C distance, we find $B=0.0766$ ($\pm 0.0005$) $cm^{-1}$. This value represents an average over all populated states, and it agrees well with the value of 0.0764 $cm^{-1}$ obtained by averaging the $B''$ values in Table VIII. If we had assumed a rigid linear structure with fixed C=C and C=O lengths of 1.2899 Å and 1.1645 Å,[26,27] respectively, then a value $B=0.0725$ $cm^{-1}$ would have resulted, which is substantially below any of the observed values.

An estimate of $\omega_7$ can be obtained from the relation[28]

$$q_t'' \approx 2B^2/\omega_7\,. \tag{3}$$

Using the values from Table VIII, Eq. (3) yields $32\pm 6$ $cm^{-1}$ for the low frequency bending mode, compared with the observed value of 22 $cm^{-1}$. The agreement is not bad considering the fact that Eq. (3) assumes a harmonic potential for $\nu_7$, while the actual potential is expected to be highly anharmonic.[15,27,29,30] The magnitude of $q_t''$ in the Δ states is expected to be $\approx 10^{-6}$ $cm^{-1}$, i.e., a factor $(B/\omega_7)$ smaller than it is in the Π states.[28] Thus, within our accuracy, the $B$ values in the Δ states should be equal, which is in agreement with the results in Table VIII.

The magnitude of the centrifugal distortion term $D$ in $C_3O_2$ appears to be anomalously large compared with other similar molecules. In $CO_2$, $CS_2$, $C_2H_2$, $C_2D_2$, and $C_2N_2$, all linear symmetric molecules, the $D$ term is given to usually better than 20% accuracy by $4B^3/\omega_s^2$, where $\omega_s$ is the lowest symmetric stretching frequency. In $C_3O_2$ the same expression (with $\omega_s=800$ $cm^{-1}$) yields a $D$ value at least a factor of ten below the observed

TABLE VII. Observed frequencies (vac. $cm^{-1}$) of the $\nu_4+2\nu_7^0 \leftarrow 2\nu_7^0$ transitions. The rms error of the fit using the molecular constants in Table VIII is $\pm 0.0019$ $cm^{-1}$ for 50 lines.

| $J$ | $R(J)$ OBS | O−C | $P(J)$ OBS | O−C |
|---|---|---|---|---|
| 2 | 1583.5863 | 0.0020 | ... | ... |
| 4 | 1583.8917 | 0.0024 | ... | ... |
| 6 | 1584.1941 | −0.0000 | ... | ... |
| 8 | 1584.4997 | 0.0009 | ... | ... |
| 10 | 1584.8048 | 0.0014 | ... | ... |
| 12 | 1585.1071 | −0.0006 | ... | ... |
| 14 | 1585.4110 | −0.0009 | ... | ... |
| 16 | 1585.7155 | −0.0004 | ... | ... |
| 18 | 1586.0180 | −0.0017 | 1580.3698 | −0.0051 |
| 20 | 1586.3236 | 0.0004 | ... | ... |
| 22 | 1586.6261 | −0.0004 | 1579.7620 | −0.0005 |
| 24 | 1586.9274 | −0.0022 | 1579.4517 | −0.0045 |
| 26 | 1587.2306 | −0.0018 | 1579.1499 | 0.0001 |
| 28 | 1587.5346 | −0.0004 | 1578.8431 | −0.0002 |
| 30 | 1587.8371 | −0.0002 | 1578.5385 | 0.0019 |
| 32 | 1588.1411 | 0.0017 | 1578.2321 | 0.0023 |
| 34 | 1588.4425 | 0.0014 | 1577.9265 | 0.0036 |
| 36 | 1588.7432 | 0.0006 | 1577.6203 | 0.0046 |
| 38 | 1589.0458 | 0.0020 | 1577.3086 | 0.0003 |
| 40 | 1589.3461 | 0.0014 | 1577.0010 | 0.0003 |
| 42 | ... | ... | 1576.6914 | −0.0013 |
| 44 | ... | ... | ... | ... |
| 46 | ... | ... | 1576.0724 | −0.0033 |
| 48 | 1590.5427 | −0.0023 | 1575.7647 | −0.0018 |
| 50 | 1590.8430 | −0.0012 | 1575.4551 | −0.0016 |
| 52 | 1591.1426 | −0.0005 | 1575.1456 | −0.0008 |
| 54 | 1591.4420 | 0.0004 | 1574.8356 | 0.0003 |
| 56 | 1591.7403 | 0.0006 | 1574.5247 | 0.0013 |
| 58 | 1592.0379 | 0.0005 | 1574.2146 | 0.0040 |
| 60 | ... | ... | 1573.8978 | 0.0010 |
| 62 | ... | ... | 1573.5797 | −0.0022 |
| 64 | ... | ... | 1573.2638 | −0.0019 |
| 66 | ... | ... | 1572.9468 | −0.0012 |
| 68 | ... | ... | 1572.6309 | 0.0021 |

TABLE VIII. Molecular constants (vac. $cm^{-1}$) for the $\nu_4\ 1 \leftarrow 0$ transitions of $^{12}C_3\,^{16}O_2$.

| Transition | $\nu_0$ | $B''$ | $B'-B''(10^{-4})$ | $D''(10^{-8})$ | $D'-D''(10^{-8})$ | $H''(10^{-12})$ | $H'-H''(10^{-12})$ |
|---|---|---|---|---|---|---|---|
| $\nu_4 \leftarrow 0^\circ$ | 1587.390 | 0.075573 | 6.450 | 4.183 | 1.928 | 0.616 | 0.192 |
| | ±0.002 | $\pm 2\times10^{-5}$ | ±0.04 | ±0.4 | ±0.3 | ±0.1 | ±0.1 |
| | | (0.075563)[a] | | (3.817)[a] | | (0.601)[a] | |
| $\nu_4+\nu_7^{1c} \leftarrow \nu_7^{1c}$ | 1580.896 | 0.076052 | 4.453 | 6.604 | 2.020 | 7.400 | 1.54 |
| | ±0.003 | $\pm 3\times10^{-5}$ | ±0.08 | ±2.0 | ±0.6 | ±4.0 | ±1.0 |
| | | (0.07605)[b] | | | | | |
| $\nu_4+\nu_7^{1d} \leftarrow \nu_7^{1d}$ | 1580.901 | 0.076414 | 5.345 | 3.460 | 1.519 | 0.849 | 0.232 |
| | ±0.003 | $\pm 3\times10^{-5}$ | ±0.06 | ±1.5 | ±0.3 | ±2.0 | ±0.2 |
| | | (0.07648)[b] | | | | | |
| $\nu_4+2\nu_7^{2c} \leftarrow 2\nu_7^{2c}$ | 1575.094 | 0.076913 | 3.961 | 4.226 | 0.453 | 1.640 | −0.276 |
| | ±0.003 | $\pm 3\times10^{-5}$ | ±0.08 | ±1.8 | ±0.4 | ±2.0 | ±0.5 |
| $\nu_4+2\nu_7^{2d} \leftarrow 2\nu_7^{2d}$ | 1575.092 | 0.076902 | 3.958 | 4.616 | −0.113 | 2.03 | −0.804 |
| | ±0.003 | $\pm 3\times10^{-5}$ | ±0.08 | ±1.8 | ±0.4 | ±2.0 | ±0.5 |
| | 1575.098[c] | | | | | | |
| $\nu_4+2\nu_7^{0} \leftarrow 2\nu_7^{0}$ | 1583.126 | 0.076327 | −0.154 | 4.829 | 0.124 | 6.25 | −0.29 |
| | ±0.003 | $\pm 3\times10^{-5}$ | ±0.04 | ±2.0 | ±0.4 | ±5.0 | ±0.5 |
| | | (0.076280)[a] | | (1.76)[a] | | (1.58)[a] | |

[a]Reference 17. [b]Assignment 2, Ref. 16. [c]From $Q$ branch.

values. This result indicates that the primary effect of centrifugal distortion in $C_3O_2$ is a straightening out of the molecule, i.e., a stiffening of the restoring force and consequent reduction in amplitude of the $\nu_7$ bending mode, rather than a stretching of the bonds.

The signs of most of the $B'-B''$ terms in $C_3O_2$ also appear to be anomalous compared with other linear molecules. For example, in the excitation of the asymmetric stretching modes $\nu_3$ of $CO_2$ or $\nu_3$ of $C_2H_2$, the $B'-B''$ terms are all negative, while in a corresponding mode $\nu_4$ of $C_3O_2$, all the $B'-B''$ terms are positive, except for the $2\nu_7^0$ state. This result suggests a strong anharmonic coupling of $\nu_4$ and $\nu_7$, leading to an increased bending mode amplitude in the $\nu_4$ excited state. The same conclusion is supported by the systematic shift of the hot bands to lower frequencies.

Carriera *et al.*[15] have determined a potential function for $\nu_7$ by fitting their far infrared and Raman spectra. It would be of interest to compare the moments of inertia calculated from their model with the data in Table VIII. Also the band contours for a number of Raman and far infrared bands can now be calculated and checked against their assignments.

## ACKNOWLEDGMENTS

The authors wish to thank Prof. K. N. Rao for sending us a listing of improved $NH_3$ line positions prior to publication. The assistance of C. M. Savage and L. P. Breitenbach in obtaining the Fourier transform spectra and of K. F. Yeung in obtaining some of the early laser spectra is gratefully acknowledged. The PbTe films used to make the lasers were grown by M. Mikkor.

[1]A recent review of diode laser spectroscopy is given by A. R. Calawa, J. Lumin. **7**, 477 (1973).
[2]K. W. Nill, F. A. Blum, A. R. Calawa, and T. C. Harman, Chem. Phys. Lett. **14**, 234 (1972).
[3]G. A. Antcliffe, S. G. Parker, and R. T. Bate, Appl. Phys. Lett. **21**, 505 (1972).
[4]F. A. Blum, K. W. Nill, P. L. Kelley, A. R. Calawa, and T. C. Harman, Science **177**, 694 (1972).
[5]G. A. Antcliffe and J. S. Wrobel, Appl. Opt. **11**, 1548 (1972).
[6]W. H. Weber, P. D. Maker, K. F. Yeung, and C. W. Peters, Appl. Opt. **13**, 1431 (1974).
[7]F. A. Blum, K. W. Nill, A. R. Calawa, and T. C. Harman, Chem. Phys. Lett. **15**, 144 (1972).
[8]W. Engler and K. W. F. Kohlrausch, Z. Phys. Chem. Abt. B **34**, 214 (1936).
[9]R. C. Lord and N. Wright, J. Chem. Phys. **5**, 642 (1937).
[10]D. A. Long, F. S. Murfin, and R. L. Williams, Proc. R. Soc. London A **223**, 251 (1954).
[11]H. D. Rix, J. Chem. Phys. **22**, 429 (1954).
[12]B. P. Stoicheff, Adv. Spectrosc. **1**, 124 (1959).
[13]F. A. Miller and W. G. Fateley, Spectrochim. Acta **20**, 253 (1964).
[14]W. H. Smith and G. E. Leroi, J. Chem. Phys. **45**, 1767 (1967).
[15]L. A. Carreira, R. O. Carter, J. R. Durig, R. C. Lord, and C. C. Milionis, J. Chem. Phys. **59**, 1028 (1973).
[16]W. J. Lafferty, A. G. Maki, and E. K. Plyler, J. Chem. Phys. **40**, 224 (1964).
[17]A. W. Mantz, P. Connes, G. Guelachvili, and C. Amiot, J. Mol. Spectrosc. **54**, 43 (1975).
[18]W. H. Weber and K. F. Yeung, J. Appl. Phys. **44**, 4991 (1973).
[19]G. P. Montgomery, Jr. and J. C. Hill, J. Opt. Soc. Am. **65**, 579 (1975).
[20]*American Institute of Physics Handbook*, edited by Dwight E. Gray (McGraw–Hill, New York, 1972), 3rd ed., Chap. 6, p. 30.
[21]J. S. Garing, H. H. Nielsen, and K. N. Rao, J. Mol. Spectrosc. **3**, 496 (1959).
[22]A listing of improved line positions was provided by K. N. Rao (private communication, Sept. 1974).
[23]E. A. Cohen and R. L. Poynter, J. Mol. Spectrosc. **53**, 131 (1974).
[24]P. D. Maker, H. Niki, C. M. Savage, and L. P. Breitenbach, *Proceedings of the Thirtieth Symposium on Molecular Structure and Spectroscopy*, Columbus, Ohio, 16–20 June, 1975, p. 150.
[25]G. Herzberg, *Infrared and Raman Spectra* (Van Nostrand,

New York, 1945), Chap. IV, p. 380.
[26]A. Almenningen, S. P. Arnesen, O. Bastiansen, H. M. Seip, and R. Seip, Chem. Phys. Lett. **1**, 569 (1968).
[27]A. Clark and H. M. Seip, Chem. Phys. Lett. **6**, 452 (1970). We have made the corrections to the data in Ref. 26 indicated in this paper.
[28]See, for example, C. H. Townes and A. L. Schawlow, *Microwave Spectroscopy* (McGraw–Hill, New York, 1955), p. 33.
[29]F. A. Miller, D. H. Lemmon, and R. E. Witkowski, Spectrochim. Acta **21**, 1709 (1965).
[30]R. L. Redington, Spectrochim. Acta Part A **23**, 1863 (1967).